Electronic Research Archive

ERA, 30 (2): 715–731.
DOI: 10.3934/era.2022038
Received: 23 September 2021
Revised: 01 November 2021
Accepted: 02 November 2021
Published: 25 February 2022

http://www.aimspress.com/journal/ERA

Research article

Spatiotemporal pattern in a neural network with non-smooth memristor

Xuerong Shi[1], Zuolei Wang[1,*] and Lizhou Zhuang[2]

[1] School of Mathematics and Statistics, Yancheng Teachers University, Yancheng 224002, China
[2] School of Chemical and Environmental, Yancheng Teachers University, Yancheng 224007, China

* **Correspondence:** Email: wzlyctc@163.com; Tel: +86-15195122720; Fax: +86-051588233882.

Abstract: Considering complicated dynamics of non-smooth memductance function, an improved Hindmarsh-Rose neuron model is introduced by coupling with non-smooth memristor and dynamics of the improved model are discussed. Simulation results suggest that dynamics of the proposed neuron model depends on the external stimuli but not on the initial value for the magnetic flux. Furthermore, a network composed of the improved Hindmarsh-Rose neuron is addressed via single channel coupling method and spatiotemporal patterns of the network are investigated via numerical simulations with no-flux boundary condition. Firstly, development of spiral wave are discussed for different coupling strengths, different external stimuli and various initial value for the magnetic flux. Results suggest that spiral wave can be developed for coupling strength $0 < D < 1$ when the nodes are provided with period-1 dynamics, especially, double-arm spiral wave appear for $D = 0.4$.External stimuli changing can make spiral wave collapse and the network demonstrates chaotic state. Alternation of initial value for the magnetic flux hardly has effect on the developed spiral wave. Secondly, formation of target wave are studied for different coupling strengths, different sizes of center area with parameter diversity and various initial value for the magnetic flux. It can be obtained that, for certain size of center area with parameter diversity, target wave can be formed for coupling strength $0 < D < 1$, while for too small size of center area with parameter diversity, target wave can hardly be formed. Change of initial value for the magnetic flux has no effect on the formation of target wave. Research results reveal the spatiotemporal patterns of neuron network to some extent and may provide some suggestions for exploring some disease of neural system.

Keywords: spatiotemporal pattern; non-smooth memristor; Hindmarsh-Rose neuron; single channel coupling method; neuron network

1. Introduction

Collective behaviors of neural network received considerable attention because of its application in many fields. It was found that various dynamics could be observed in physical, chemical, and biological systems, from which it can be believed that numerical investigation could be feasible to explore some main properties of nonlinear dynamical systems.

As one sort of collective behavior, synchronization of neural network was investigated via various aspects and many results have been obtained. Synchronization transitions induced by information transmission delay and coupling strength in scale-free neuronal networks with different average degrees and scaling exponents were revealed and it can be known that delay plays a more subtle role than coupling strength [1]. Synaptic effect on the excitement and synchronization of synaptic coupled neuronal networks are discussed by a modified Oja learning rule and it was found that, synaptic learning can suppress the over-excitement and is helpful for realizing synchronization [2]. Synchronization transitions of bursting oscillations dependent on the information transmission delay over scale-free neuronal networks with attractive and repulsive coupling was explored and it was shown that the change of delay can promote or impair spatiotemporal synchrony [3]. Synchronization of a modified bursting Hodgkin-Huxley neuronal model is studied in various conditions and it can be obtained that various synchronizations can be achieved via different kinds of synapses [4]. Finite-time projective synchronization of memristor-based neural networks with leakage and time-varying delays was concerned and two types of projective synchronizations of were reached with several stability conditions being presented [5]. Inhibitory synchronization inspired by firing rate in E/I neuronal networks was discussed and it was discovered that firing rate contrast enhancement may play an important role for inhibitory synchronization [6].

Simultaneously, as two typical regular phenomena of spatiotemporal pattern, spiral wave and target wave attracted much attention in neuroscience. Spiral wave, which can be formed when system is far away from stable state, can be found in many systems. Existing results indicated that spiral wave may be induced by parameter heterogeneity [7], broken target wave [8], autapses in the media [9], partial channel blocking [10], probability of long-range connection [11], state of the single Hindmarsh-Rose neuron [12] and appropriate initial state [13]. Target wave can emerge when dissipative system is far from equilibrium point [14]. It is found that, various regular waves can be produced with the change of autapse number [15] and coherence of spiral waves can be enhanced by time-delay [16]. Abovementioned results suggest that spatiotemporal patterns of neural network can be affected by many factors.

Recently, the influence of electromagnetic induction on spatiotemporal patterns of neural network comes to researcher's notice. For instance, complex spatiotemporal patterns of neuronal network exposed to external electromagnetic field were discovered [17]; formation of spiral wave in memristor-based Hindmarsh-Rose neural network was announced [18]. The results indicate that, considering electromagnetic induction, neural networks demonstrated complicated spatiotemporal patterns. It is noted that, existing results are mainly about neural networks with smooth memristor. But in real application, smooth memristor sometimes will cause DC drift, to avoid this phenomenon, non-ideal voltage controlled memristor is introduced [19]. Meanwhile, as a circuit device, memristor denotes the relationship between magnetic flux and electric charge, which can show non-smooth characteristics when the relationship is discontinuous. Factually, non-smooth memristor widely exists in many fields and can induce complicated dynamics [20]. However, spatiotemporal pattern of neural network with

non-smooth memristor was hardly reported, the complex behavior for both single neuron and neural network with non-smooth memristor is worthy of in-depth study and discussion.

To further explore the spatiotemporal pattern in neural network under different electromagnetic induction, spatiotemporal pattern in a network composed of Hindmarsh-Rose neurons with non-smooth memristor is to be investigated. Other parts of this paper are arranged as follows. Hindmarsh-Rose neuron with non-smooth memristor along with its dynamical behavior is depicted in Section 2. In Section 3, a neural network is constituted by the revised Hindmarsh-Rose neuron model and spatiotemporal pattern of the network is discussed under different conditions. Section 4 gives some conclusions.

2. Hindmarsh-Rose neuron coupled by non-smooth memristor

In neural system, neurons receive or transmit signals via synapses. Therefore, synaptic property has much effect on the electrical activity of neuron or neural network. As a matter of fact, information transmission between neurons often appears discontinuous. To understand and master the dynamics in this case, a kind of non-smooth memristor is used to simulate the synapse of Hindmarsh-Rose neuron and a revised Hindmarsh-Rose neuron model is proposed in this section.

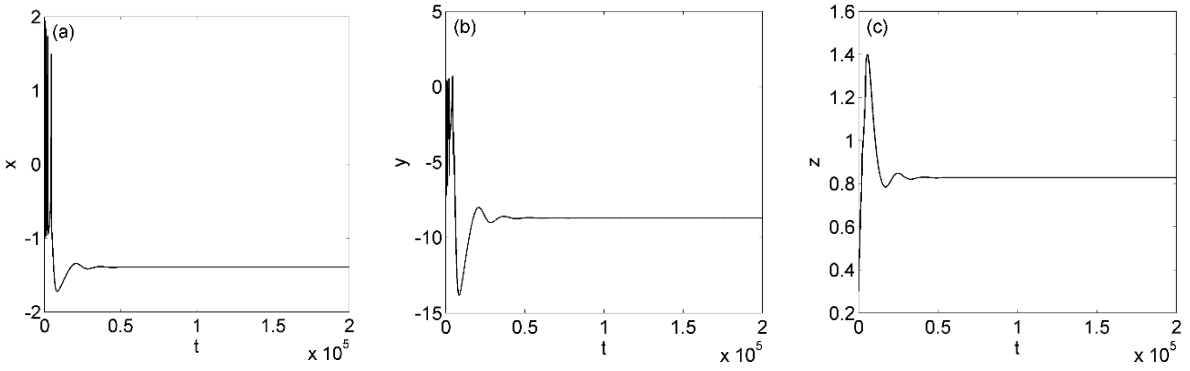

Figure 1. Equilibrium point of system (2) when I_{ext}=1.0. (a–c) Sampled time series of variables, (a) Time series of x; (b) Time series of y; (c) Time series of z.

A non-smooth memristive [19] is considered as

$$W(\varphi)=\alpha+3\beta|\varphi|, \tag{1}$$

which is non-ideal voltage controlled memristor with absolute value nonlinearity, where α and β are two positive memristor parameters, φ is internal state variable of voltage-controlled memristive. And then, Hindmarsh-Rose neuron with non-smooth memristor can be depicted as

$$\begin{cases} \dot{x}=y-ax^3+bx^2-z+I_{ext}-k_1(\alpha+3\beta|w|)x \\ \dot{y}=c-dx^2-y \\ \dot{z}=r\left[S\left(x+1.56\right)-z\right] \\ \dot{w}=x-k_2w \end{cases}, \tag{2}$$

where x represents membrane potential of neuron, y means the exchange of ions in neuron membrane, z denotes adaption current and w describes the magnetic flux across membrane. $\alpha+3\beta|w|$ is the memory conductance of memristor used to describe the coupling between magnetic flux and membrane potential of neuron. $-k_2 w$ is defined as the effect of self-inductance with k_2 being the gain dependent on the media. a, b, c, d, r, S, k_1, k_2, α and β are the parameters which govern the dynamics of the neural system. I_{ext} is external forcing current.

When system parameters are chosen as $a=1.0$, $b=3.0$, $c=1.0$, $d=5.0$, $r=0.006$, $S=4.0$, $\alpha=0.4$, $\beta=0.01$, $k_1=0.01$, $k_2=6.5$ and initial value is $x_0=(-1.3,0.5,0.3,0.1)$, system (2) can show diversity in electrical activity with external forcing current I_{ext} varying. For example, when I_{ext}=1.0, 1.3, 2.9, sampled time series of neuron model (2) can be calculated and depicted in Figures 1–3, from which it can be known that, with external forcing current changing, system (2) appears different electrical activities. Bifurcation diagram (Figure4) confirms the result as demonstrated in Figures 1–3.

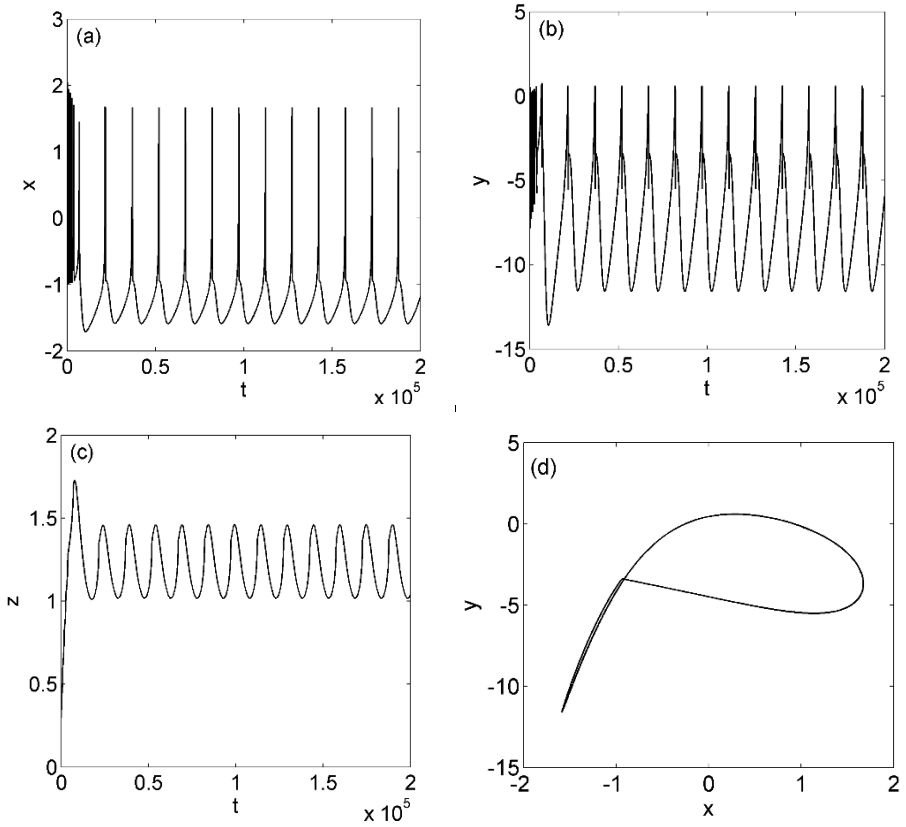

Figure 2. Periodic-1 dynamics of system (2) when I_{ext}=1.3. (a–d) Sampled time series and phase portrait, (a) Time series of x; (b) Time series of y; (c) Time series of z; (d) Phase portrait in x-y plane.

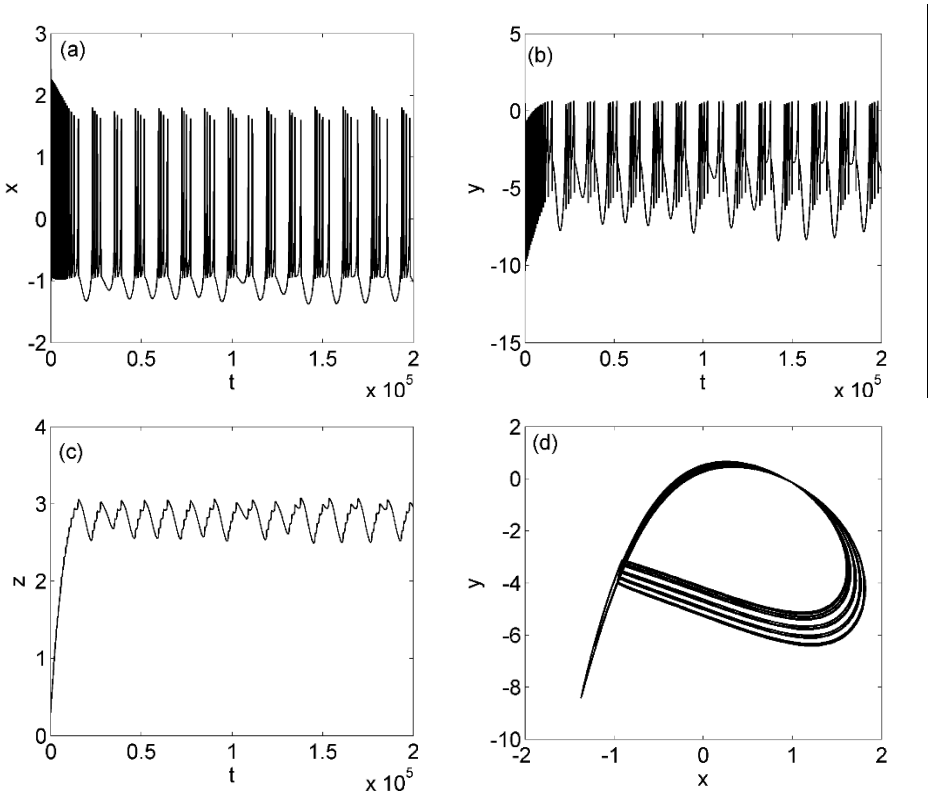

Figure 3. Chaotic dynamics of system (2) when $I_{ext} = 2.9$. (a–d)Sampled time series and phase portrait, (a) Time series of x; (b) Time series of y; (c) Time series of z; (d) Phase portrait in x-y plane.

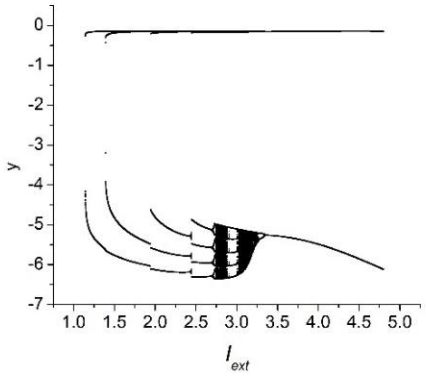

Figure 4. Bifurcation diagram. Dynamical behaviors of variable y (Poncare section at $x=1$) in system (2) with bifurcation parameter I_{ext} for $a=1.0$, $b=3.0$, $c=1.0$, $d=5.0$, $r=0.006$, $S=4.0$, $\alpha=0.4$, $\beta=0.01$, $k_1=0.01$, $k_2=6.5$ and initial value $x_0=(-1.3,0.5,0.3,0.1)$.

3. Spatiotemporal pattern of Hindmarsh-Rose neural network with non-smooth memristor

To discuss the collective behavior of neural network composed of Hindmarsh-Rose neuron with non-smooth memristor, the network with nearest-neighbor coupling via single channel is presented as

$$\begin{cases} \dot{x}_{ij} = y_{ij} - ax_{ij}^3 + bx_{ij}^2 - z_{ij} + I_{ext} - k_1(\alpha + 3\beta|w_{ij}|)x_{ij} \\ \quad\quad +D(x_{i-1j} + x_{i+1j} + x_{ij+1} + x_{ij-1} - 4x_{ij}) \\ \dot{y}_{ij} = c - dx_{ij}^2 - y_{ij} \\ \dot{z}_{ij} = r\left[S\left(x_{ij} + 1.56\right) - z_{ij}\right] \\ \dot{w}_{ij} = x_{ij} - k_2 w_{ij} \end{cases}, \tag{3}$$

where D is coupling coefficient between adjacent neurons, a, b, c, d, r, S, I_{ext}, k_1, k_2, α and β are defined the same as in system (2). It is supposed that the parameter values of neurons in network (3) are all the same. Therefore, all the nodes in the network are identical. For simplicity, it is assumed that network (3) is composed of 200 × 200 neurons, which are evenly distributed in a two-dimensional lattice. And then spatiotemporal pattern of the addressed neural network is to be explored.

3.1. Spiral wave and its collapse

In network (3), choose $a = 1.0$, $b = 3.0$, $c = 1.0$, $d = 5.0$, $r = 0.006$, $S = 4.0$, $I_{ext} = 1.3$, $\alpha = 0.4$, $\beta = 0.01$, $k_1 = 0.01$, $k_2 = 6.5$, with which each node presents period-1 bursting, and spiral wave can be formed for coupling intensity $0 < D < 1$. To illustrate this result, D is taken as several different values and dynamical behaviors of network (3) are simulated (Figures 5–8) considering no-flux boundary condition and initial value (−1.31742, −7.67799, 1.1302, 1.302), which indicate that, regular spiral wave can be induced and tends to be stable over time. With coupling intensity increasing, spiral wave can be formed faster. Especially, for $D = 0.4$, double-arm spiral wave can be observed (Figure 6). That is to say, by selecting suitable parameters, spiral wave can be developed in neural network (3) when the nodes exhibit period-1 bursting.

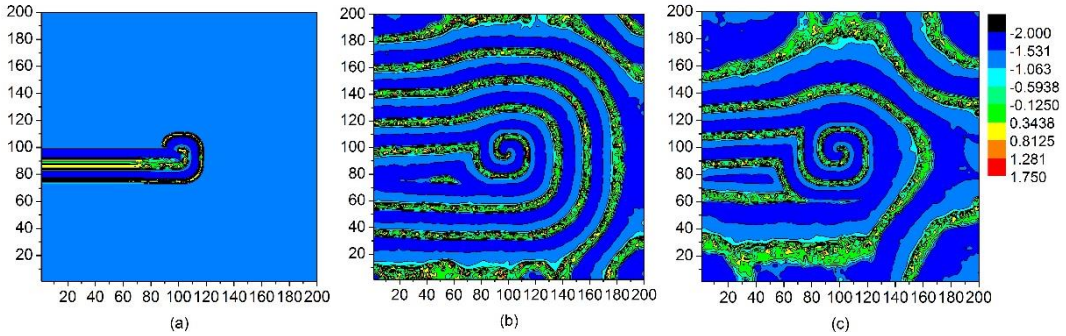

Figure 5. Formation of spiral wave in network (3) with $D = 0.2$ and $I_{ext} = 1.3$. (a–c) The developed spiral wave states of membrane potential x at different time units, (a) At $t = 300$ time units; (b) At $t = 4000$ time units; (c) At $t = 8000$ time units.

To further explore the development of spiral wave in network (3), external forcing current is considered as $I_{ext} = 1.0$ (each node tends to be stable at one point), $I_{ext} = 1.5$ (each node presents period-2 bursting), $I_{ext} = 2.1$ (each node shows period-3 bursting), $I_{ext} = 2.5$ (each node demonstrates period-4 bursting), $I_{ext} = 2.8$ (each node appears chaotic bursting) and the simulation results with no-flux boundary condition and initial value (−1.31742, −7.67799, 1.1302, 1.302) are depicted in Figure 9, which means that, when $I_{ext} = 1.0, 1.5, 2.1, 2.5$, spiral wave cannot form, while roaming spiral wave

can appear for I_{ext}=2.8. It means that changing of external forcing current can make spiral wave in network (3) collapse and demonstrates chaotic state.

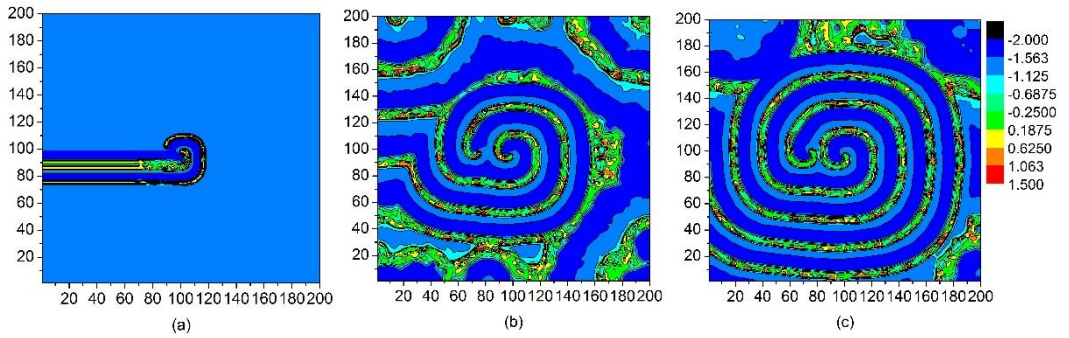

Figure 6. Formation of double-arm spiral wave in network (3) with $D=0.4$ and I_{ext}=1.3. (a–c) The developed double-arm spiral wave state of membrane potential x at different time units, (a) At $t=300$ time units; (b) At $t=4000$ time units; (c) At $t=8000$ time units.

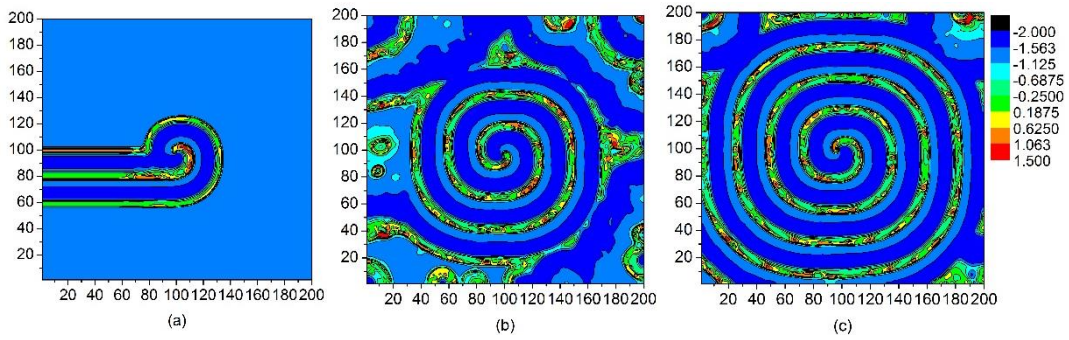

Figure 7. Formation of spiral wave in network (3) with $D=0.5$ and I_{ext}=1.3. (a–c) The developed spiral wave state of membrane potential x at different time units, (a) At $t=300$ time units; (b) At $t=4000$ time units; (c) At $t=8000$ time units.

From Figures 5–9, it can be known that dynamics of the nodes in network (3) plays an important role for developed spiral wave. To investigate the effect of initial value for the magnetic flux on spatial patterns of network (3), the effect of initial value for the magnetic flux on the dynamics of neuron system (2) is discussed. Choose $a=1.0$, $b=3.0$, $c=1.0$, $d=5.0$, $r=0.006$, $S=4.0$, I_{ext}=1.3, $\alpha=0.4$, $\beta=0.01$, $k_1=0.01$, $k_2=6.5$, numerical simulations indicate that initial value for the magnetic flux hardly has effect on the dynamics of system (2). Given examples, for initial value $x_0=(-1.3,0.5,0.3,w_0)$ with w_0 chosen as 0, 10, and sampled time series as well as phase portrait are calculated and depicted in Figure 10. Furthermore, the effect of initial value for the magnetic flux on the development of spiral wave is investigated via numerical simulations with no-flux boundary condition. By way of illustration, select $a=1.0$, $b=3.0$, $c=1.0$, $d=5.0$, $r=0.006$, $S=4.0$, I_{ext}=1.3, $\alpha=0.4$, $\beta=0.01$, $k_1=0.01$, $k_2=6.5$, $D=0.5$, I_{ext}=1.3, initial value is taken as $x_0=(-1.31742,-7.67799,1.1302,w_0)$ with w_0 chosen as 0 and 10, spatial patterns of network (3) are illustrated in Figure 11. Compared Figure 11 with Figure 7, it can be obtained that, initial value for the magnetic flux has little effect on transition of spatial patterns

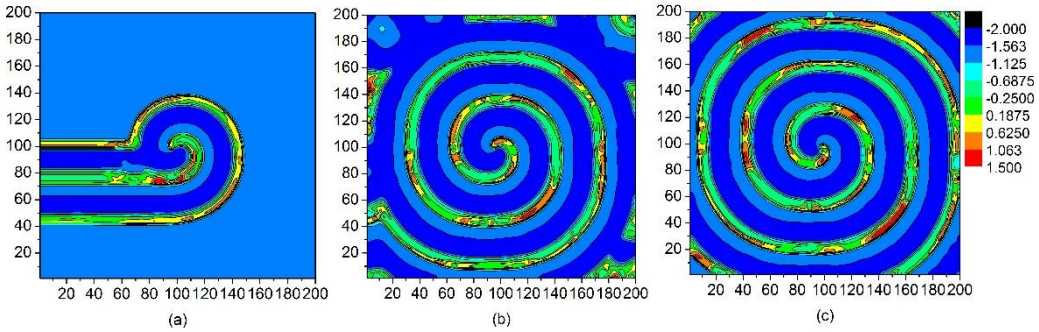

Figure 8. Formation of spiral wave in network (3) with $D=0.9$ and I_{ext}=1.3. (a–c) The developed spiral wave state of membrane potential x at different time units, (a) At $t=300$ time units; (b) At $t=4000$ time units; (c) At $t=8000$ time units.

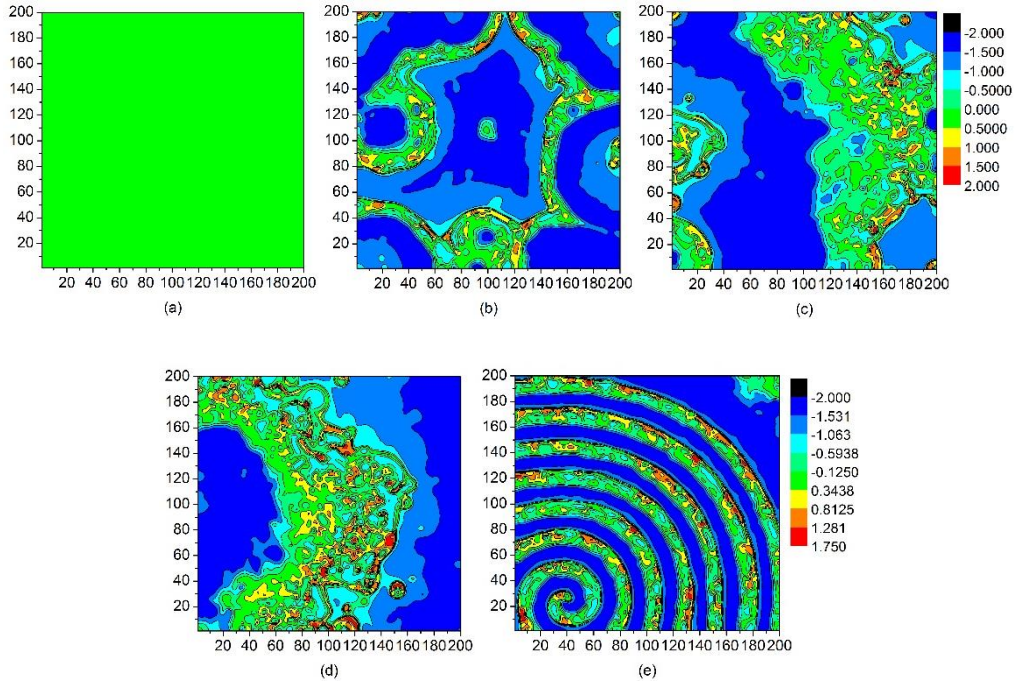

Figure 9. Collapse and roaming of spiral wave in network (3) with $D=0.9$ and different I_{ext}. (a–d) Spatiotemporal pattern state of membrane potential x at $t=8000$ time units for various values of I_{ext}, (a) For I_{ext}=1.0; (b) For I_{ext}=1.5; (c) For I_{ext}=2.1; (d) For I_{ext}=2.5; (e) For I_{ext}=2.8.

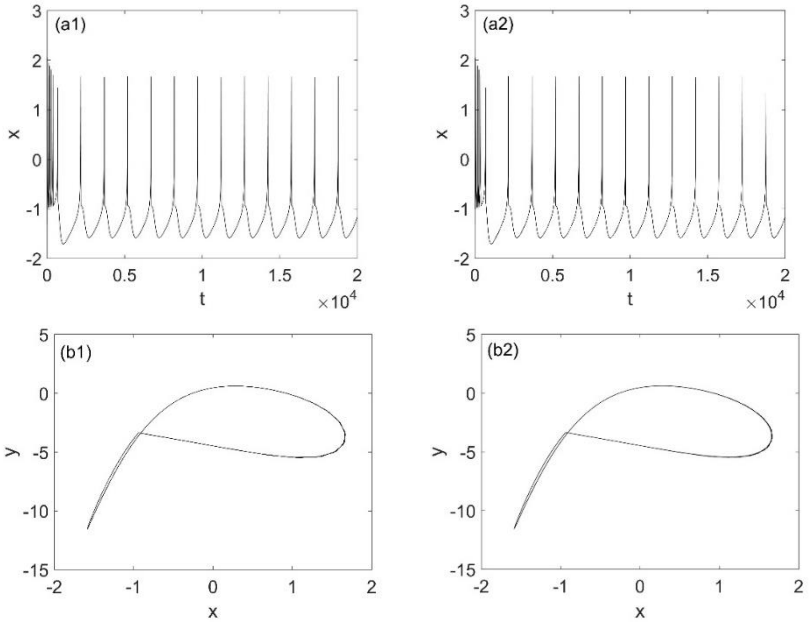

Figure 10. No effect of initial value for the magnetic flux on the dynamics of neuron system (2) for I_{ext}=1.3. (a_1-a_2) mean time series of membrane potential x and (b_1-b_2) denote phase portrait in x-y plane for different values of w_0, (a_1) Time series of x when w_0=0; (a_2) Time series of x when w_0=10; (b_1) Phase portrait when w_0=0; (b_2) Phase portrait when w_0=10.

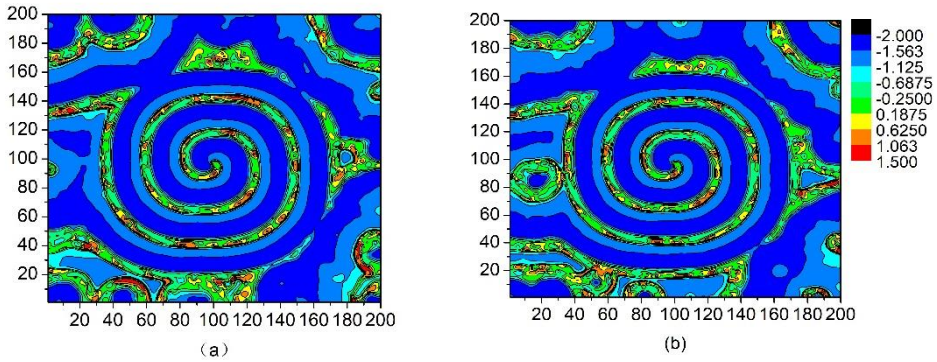

Figure 11. Little effect of initial value for the magnetic flux on development of spiral wave in network (3) with $D=0.5$ and I_{ext}=1.3. (a-b) Developed spiral wave of membrane potential x at $t=4000$ time units for different initial values of magnetic flux, (a) For $\omega_0=0$; (b) For $\omega_0=10$.

3.2. Target wave and its collapse

In this section, choose $a=1.0$, $b=3.0$, $c=1.0$, $d=5.0$, $r=0.006$, $S=4.0$, I_{ext}=1.0, $\alpha=0.4$, $\beta=0.01$, $k_1=0.01$, $k_2=6.5$,with which neuron system (2) stabilizes to an equilibrium point, target wave of neural network (3) is to be investigated.

Firstly, target wave induced by local heterogeneity of parameter is discussed with no-flux

boundary condition. For this end, parameter a is set as 0.9 for center area (9 × 9) nodes while other nodes are selected as $a=1.0$. Namely, in neural network (3), the nodes in center area show period-1 bursting (Figure 12) while other nodes stabilize to an equilibrium point (Figure 1) with initial value $x_0=(-1.3,0.5,0.3,0.1)$. Choose $D=0.3$, 0.5 and 0.9, spatial patterns of network (3) are calculated with initial value (−1.31742, −7.67799, 1.1302, 1.302) and plotted in Figures 13–15, which indicate that stable target wave can be produced. Simultaneously, with D increasing, target wave becomes sparser and earlier to occupy the network completely. Above results suggest that, if I_{ext}=1.0, for $0<D<1$, target wave will be induced by local heterogeneity when centre area is with 9 × 9 nodes.

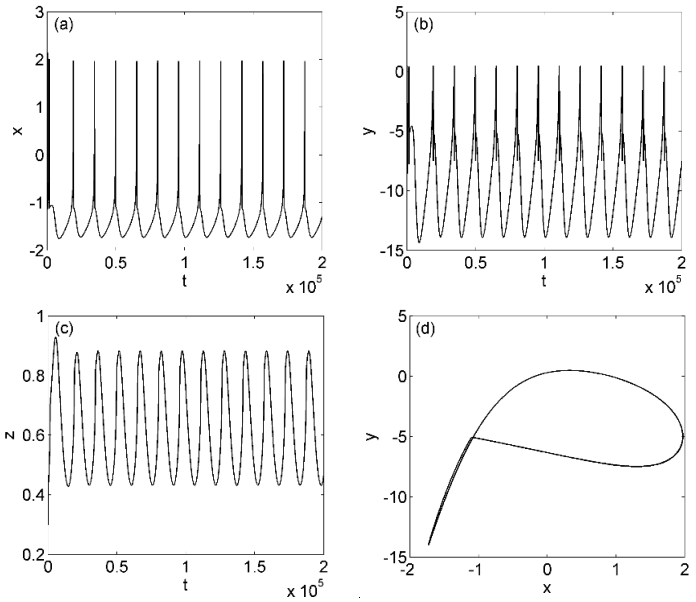

Figure 12. Period-1 dynamics of system (2) with $a=0.9$, $b=3.0$, $c=1.0$, $d=5.0$, $r=0.006$, $S=4.0$, I_{ext}=1.0, $\alpha=0.4$, $\beta=0.01$, $k_1=0.01$, $k_2=6.5$. (a–d) Sampled time series and phase portrait of the nodes in the center area (9×9) of network (3), (a) Sampled time series of x; (b) Sampled time series of y; (c) Sampled time series of z; (d) Phase portrait in x-y plane.

Factually, when the center area with parameter diversity is too small, the local heterogeneity of parameter can hardly induce target wave in neural network (3). To illustrate this phenomenon, center area is chosen as 3 × 3 nodes, the dynamical behaviors of network (3) are simulated with no-flux boundary condition and initial value (−1.31742, −7.67799, 1.1302, 1.302) (see Figure 16), from which it is obvious to know that, when the size of center area is two small, target wave can hardly be formed even for large coupling strength. The reason may be that the energy change caused by parameter heterogeneity is too small to induce continuous diffusion outward.

To further explore the effect of size of center area with local parameter heterogeneity on the formation of target wave, the center area with local heterogeneity of parameter is chosen as 11 × 11, 15 × 15, respectively, with $a=0.9$ for center nodes while $a=1.0$ for other nodes. Dynamical behaviors of network (3) are calculated with no-flux boundary condition and initial value (−1.31742, −7.67799, 1.1302, 1.302) for different coupling intensity and given in Figures 17 and 18, which demonstrate that, stable target wave can be induced by parameter heterogeneity for coupling intensity $0<D<1$. In addition, it can be known that, the larger the coupling intensity is, target wave can be formed easily.

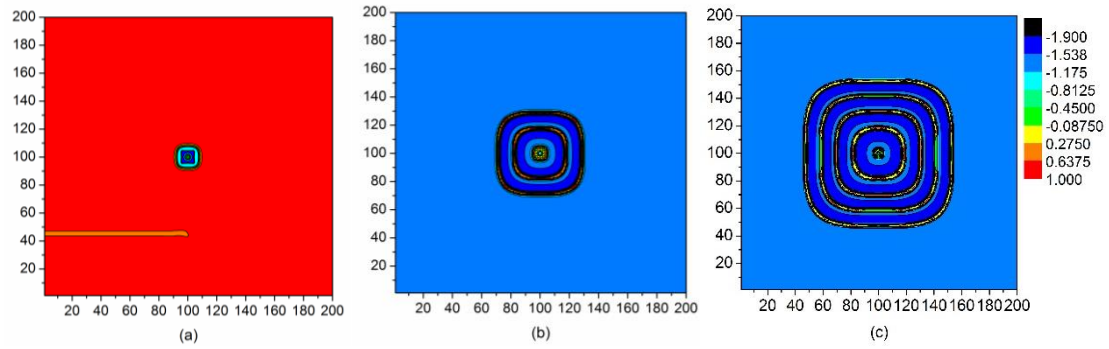

Figure 13. Formation of stable target wave when I_{ext}=1.0, $D=0.3$. (a–c) Developed target wave in network (3) induced by local heterogeneity of parameter a with center area (9 × 9) nodes $a=0.9$ and other nodes $a=1.0$ at different time units, (a) At $t=300$ time units; (b) At $t=800$ time units; (c) At $t=1200$ time units.

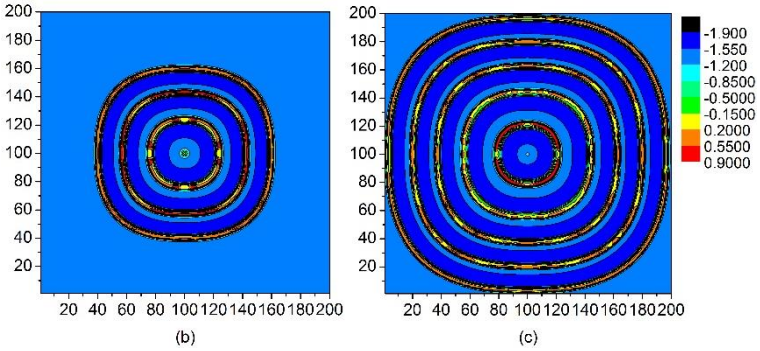

Figure 14. Formation of stable target wave when I_{ext}=1.0, $D=0.5$. (a–c) Developed target wave in network (3) induced by local heterogeneity of parameter a with center area (9×9) nodes $a=0.9$ and other nodes $a=1.0$ at different time units, (a) At $t=300$ time units; (b) At $t=800$ time units; (c) At $t=1200$ time units.

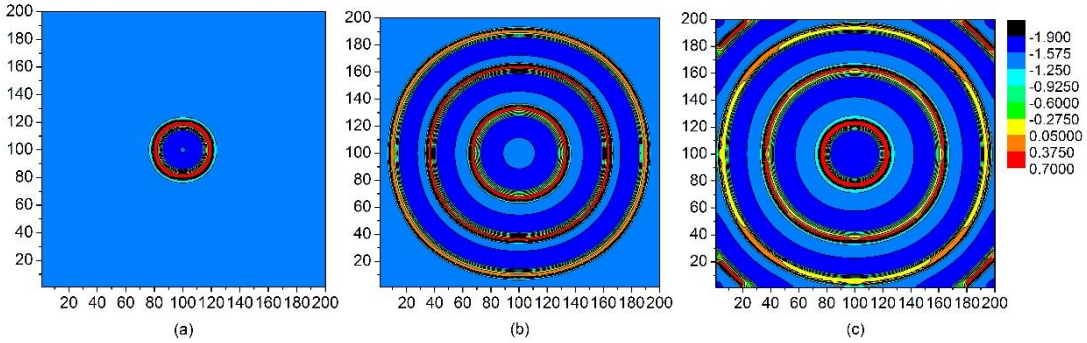

Figure 15. Formation of stable target wave when I_{ext}=1.0, $D=0.9$. (a–c) Developed target wave in network (3) induced by local heterogeneity of parameter a with center area (9 × 9) nodes $a=0.9$ and other nodes $a=1.0$ at different time units, (a) At $t=300$ time units; (b) At $t=800$ time units; (c) At $t=1200$ time units.

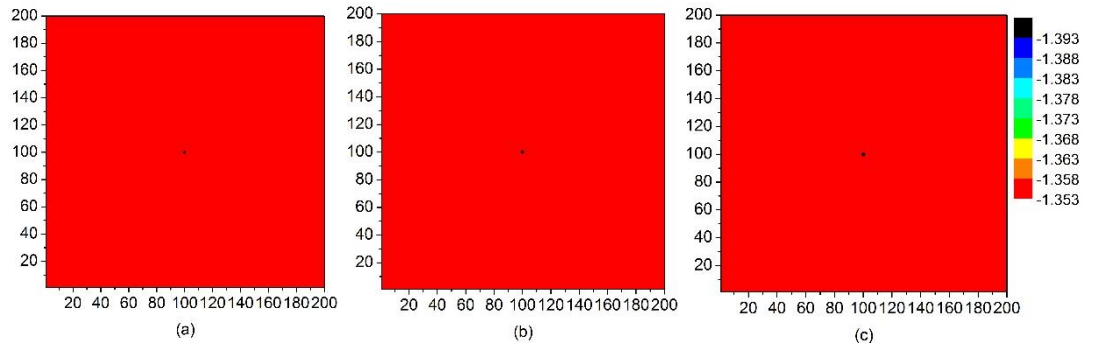

Figure 16. No regular spatial pattern can be formed when center area is chosen 3×3 nodes. (a–c) Spatiotemporal pattern state of network (3) for nodes in center area with $a=0.9$ and other nodes with $a=1.0$ at t=2500 time units for different coupling intensity, (a) $D=0.4$; (b) $D=0.7$; (c) $D=0.9$.

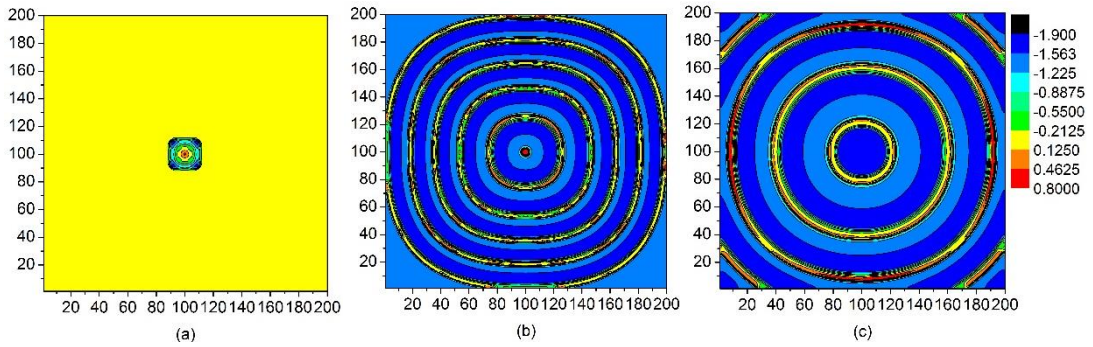

Figure 17. Formation of stable target wave with center area (11×11) nodes. (a–c) Developed target wave in network (3) induced by local heterogeneity of parameter a with center area nodes $a=0.9$ and other nodes $a=1.0$ at $t=800$ time units for different value of coupling strength D when I_{ext}=1.0, (a) $D=0.2$; (b) $D=0.5$; (c) $D=0.9$.

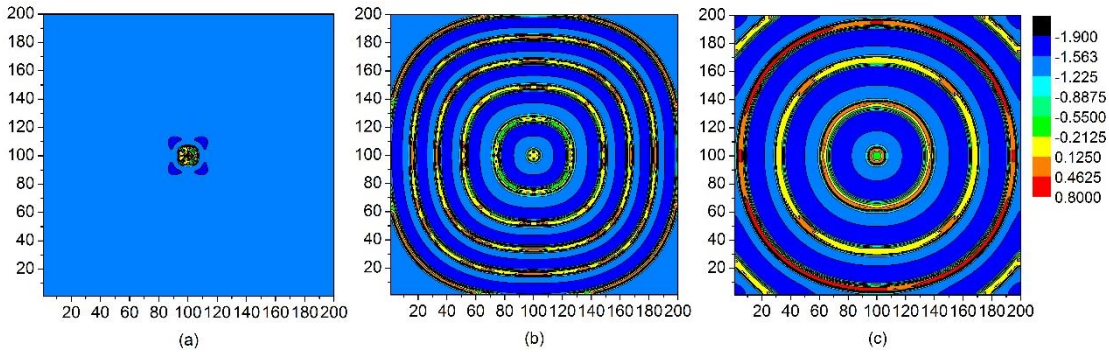

Figure 18. Formation of stable target wave with center area (15×15) nodes. (a–c) Developed target wave in network (3) induced by local heterogeneity of parameter a with center area nodes $a=0.9$ and other nodes $a=1.0$ at $t=1200$ time units for different value of coupling strength D when I_{ext}=1.0, (a) $D=0.2$; (b) $D=0.5$; (c) $D=0.9$.

Secondly, the effect of external forcing current on the spatiotemporal pattern is discussed via numerical simulations with no-flux boundary condition and initial value (−1.31742, −7.67799, 1.1302,

1.302). Center area is chosen as 9×9 nodes. Parameter a is selected as 0.9 for centre area nodes while $a=1.0$ for other nodes. Choose I_{ext}=1.3, $D=0.5$ and 0.9, respectively, corresponding spatiotemporal pattern of neural network (3) are characterized in Figures 19 and 20, which indicate that, local heterogeneity of parameter can delay the development of spiral wave temporarily. But spiral wave finally comes into formation. Namely, spiral wave can be formed in the competition of target wave and spiral wave. Larger coupling intensity is helpful for inducing spiral wave. Then, take I_{ext}=1.5, 2.5, 2.8, spatiotemporal patterns of network (3) appear chaotic (Figures 21 and 22) over time.

From Figures 19–22, it is easy to know that, when the nodes in centre area appear period-1 dynamics, parameter heterogeneity can induce stable spiral wave, but when the nodes in centre area are in multiple-period or chaotic state, parameter heterogeneity cannot induce spiral wave.

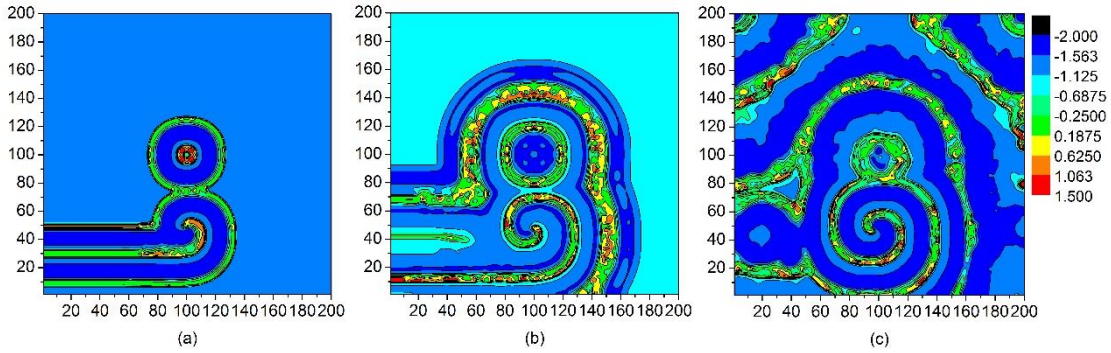

Figure 19. Competition of spiral wave and target wave for $D=0.5$ and I_{ext}=1.3. (a–c) Spatiotemporal pattern state of network (3) at different time units when center area (9×9) nodes with $a=0.9$ and other nodes with $a=1.0$, (a) At $t=300$ time units, (b) At $t=800$ time units, (c) At $t=2500$ time units.

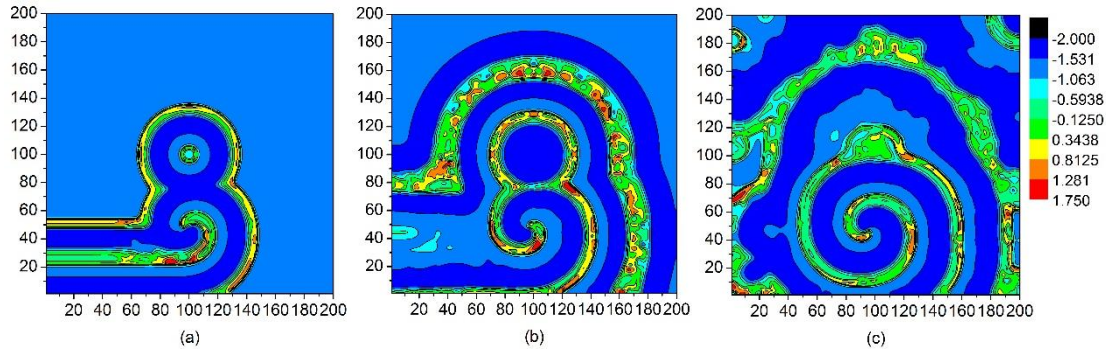

Figure 20. Competition of spiral wave and target wave for $D=0.9$ and I_{ext}=1.3. (a–c) Spatiotemporal pattern state of network (3) at different time units when center area (9×9) nodes with $a=0.9$ and other nodes with $a=1.0$, (a) At $t=300$ time units, (b) At $t=800$ time units, (c) At $t=2500$ time units.

Thirdly, by numerical simulation with no-flux boundary condition, we can draw a conclusion that initial value for the magnetic flux has no effect on the developed target wave. To illustrate this result, choose initial value $x_0=(-1.31742,-7.67799,1.1302,w_0)$ with w_0=0, 10, and center area 11 × 11 nodes,

spatiotemporal pattern of network (3) are given in Figure 23. Compared Figure 23 with Figure 14, we can conclude that the development of target wave could not be affected by the change of initial value for the magnetic flux.

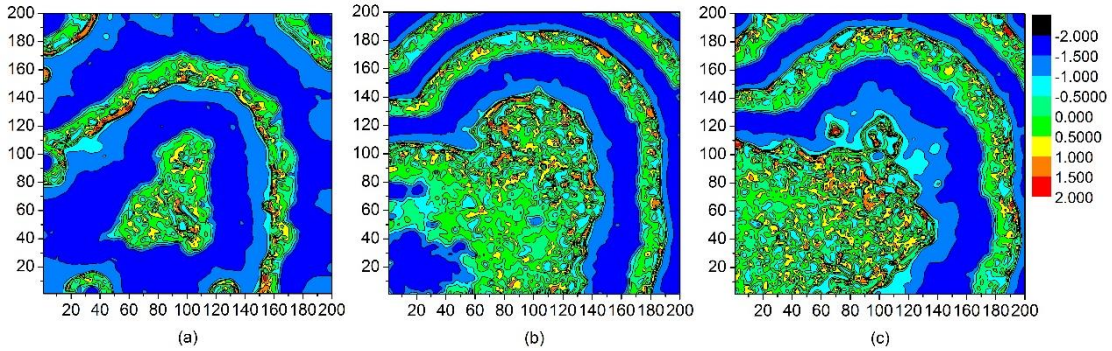

Figure 21. Chaotic behavior induced by change of external forcing current with coupling strength $D = 0.5$. (a–c) Spatiotemporal pattern state of network (3) at $t = 2500$ time units for various values of I_{ext}, (a) I_{ext}=1.5; (b) I_{ext}=2.5; (c) I_{ext}=2.8.

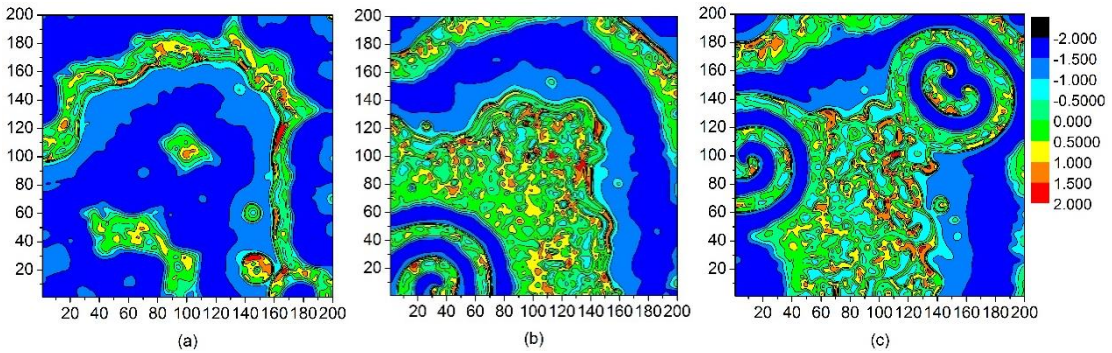

Figure 22. Chaotic behavior induced by change of external forcing current with coupling strength $D = 0.9$. (a–c) Spatiotemporal pattern state of network (3) at $t = 2500$ time units for various values of I_{ext}, (a) I_{ext}=1.5; (b) I_{ext}=2.5; (c) I_{ext}=2.8.

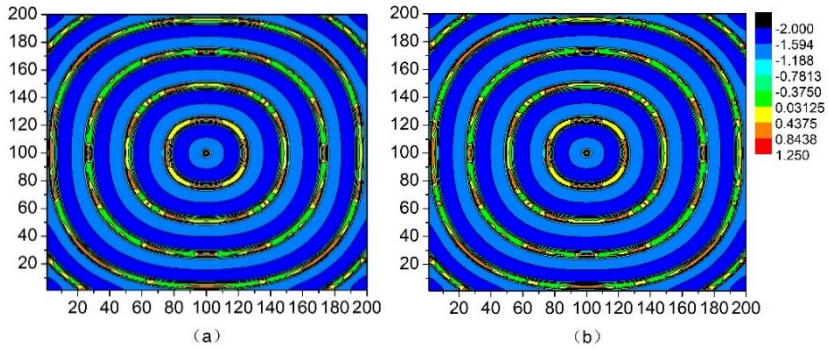

Figure 23. Initial value for the magnetic flux has no effect on development of target wave in network (3) with center area (11 × 11) nodes. (a-b) Developed target wave of membrane potential x at $t = 2500$ time units with $D = 0.5$ and I_{ext}=1.0 being used for different initial values of magnetic flux, (a) For $\omega_0 = 0$; (b) For $\omega_0 = 10$.

4. Conclusions

Considering the electromagnetic environment which neural system is in, Hindmarsh-Rose neuron model with non-smooth memristor is presented as well as its dynamics being depicted and a neural network is constituted based on it. Then, spatiotemporal patterns of the proposed network are investigated. Some results are acquired.

Firstly, stable spiral wave can be developed for coupling intensity $0 < D < 1$ when the nodes in the network is provided with period-1 bursting. The dynamics of nodes changing into multiple-period or chaos can make spiral wave collapse and hardly can be formed. Secondly, if the size of center area with local heterogeneity of parameter is large enough, when the nodes in centre area are in period-1 bursting state while other nodes converge to equilibrium point, local heterogeneity of parameter a can induce stable target wave in the addressed neural network. The change of external forcing current can also make target wave collapse. Thirdly, when the nodes in centre area are in period-2 bursting state while other nodes are in period-1 state, by setting parameter with local heterogeneity, an interesting phenomenon can be observed that spiral wave can form in the competition of target wave and spiral wave. But the increasing of external forcing current can destroy the development of spiral wave even for large coupling intensity. Additionally, whether the dynamics of the proposed neuron model or the spatiotemporal patterns of the addressed neuron network does not depend on the initial value for the magnetic flux.

The findings can provide additional insights into the pattern dynamics of networks, which is relevant to many physical, chemical, and biological systems.

Acknowledgments

The authors express sincerely appreciation to the anonymous reviewers for their efforts in reviewing the manuscript.

This work is funded by National Natural Science Foundation of China (Grant Nos. 11872327 and 51777180) and Natural Science Research Project of Jiangsu Colleges and Universities (20KJA190001).

Conflict of interest

The authors declare that they have no conflict of interest.

References

1. Q. Y. Wang, M. Perc, Z. S. Duan, G. R. Chen, Synchronization transitions on scale-free neuronal networks due to finite information transmission delays, *Phys. Rev. E*, **80** (2009), 026206. https://doi.org/10.1103/PhysRevE.80.026206
2. F. Han, M. Wiercigroch, J. A. Fang, Z. J. Wang, Excitement and synchronization of small-world neuronal networks with short-term synaptic plasticity, *Int. J. Neural Syst.*, **21** (2011), 415–425. https://doi.org/10.1142/S0129065711002924
3. Q. Y. Wang, G. R. Chen, M. Perc, Synchronous bursts on scale-free neuronal networks with attractive and repulsive coupling, *Plos One*, **6** (2011), e15851. https://doi.org/10.1371/journal.pone.0015851
4. F. Han, Z.J. Wang, Y. Du, X.J. Sun, B. Zhang, Robust synchronization of bursting Hodgkin-

Huxley neuronal systems coupled by delayed chemical synapses, *Int. J. Nonlin. Mech.*, **70** (2015), 105–111. https://doi.org/10.1016/j.ijnonlinmec.2014.10.010
5. X. L. Qin, C. Wang, L. X. Li, H. P. Peng, Y. X. Yang, L. Ye, Finite-time projective synchronization of memristor-based neural networks with leakage and time-varying delays, *Physica A*, **531** (2019), 121788. https://doi.org/10.1016/j.physa.2019.121788
6. F. Han, X. C. Gu, Z. J. Wang, H. Fan, J. F. Cao, Q.S. Lu, Global firing rate contrast enhancement in E/I neuronal networks by recurrent synchronized inhibition, *Chaos*, **28** (2018), 106324. https://doi.org/10.1063/1.5037207
7. D. H. He, G. Hu, M. Zhan, W. Ren, Z. Gao, Pattern formation of spiral waves in an inhomogeneous medium with small-world connections, *Phys. Rev. E*, **65** (2002), 055204. https://doi.org/10.1103/PhysRevE.65.055204
8. H. X. Qin, J. Ma, C. N. Wang, Y. Wu, Autapse-induced spiral wave in network of neurons under noise, *Plos One*, **9** (2014), e100849. https://doi.org/10.1371/journal.pone.0100849
9. H. X. Qin, Y. Wu, C. N. Wang, J. Ma, Emitting waves from defects in network with autapses, *Commun. Nonlinear Sci.*, **23** (2015), 164–174. https://doi.org/10.1016/j.cnsns.2014.11.008
10. X.Y. Wu, J. Ma, The formation mechanism of defects, spiral wave in the network of neurons, *Plos One*, **8** (2013), e55403. https://doi.org/10.1371/journal.pone.0055403
11. J. Ma, Y. Wu, N. J. Wu, H. Y. Guo, Detection of ordered wave in the networks of neurons with changeable connection, *Sci. China Phys. Mech.*, **56** (2013), 952–959. https://doi.org/10.1007/s11433-013-5070-0
12. P. Wang, Q. Y. Li, G. N. Tang, Spontaneous generation of spiral wave in the array of Hindmarsh-Rose neurons, *Acta Phys. Sin-Ch Ed.*, **67** (2018), 030502. https://doi.org/10.7498/aps.67.20172140
13. C. N. Wang, J. Ma, J. Tang, Y. L. Li, Instability and death of spiral wave in a two-dimensional array of Hindmarsh-Rose neurons, *Commun. Theor. Phys.*, **53** (2010), 382–388. https://doi.org/10.1088/0253-6102/53/2/32
14. Y. Xu, W. Y. Jin, J. Ma, Emergence and robustness of target waves in a neuronal network, *Int. J. Mod. Phys. B*, **29** (2015), 1550164. https://doi.org/10.1142/S0217979215501647
15. H. X. Qin, J. Ma, C. N. Wang, R. T. Chu, Autapse-induced target wave, spiral wave in regular network of neurons, *Sci. China Phys. Mech.*, **57** (2014), 1918–1926. https://doi.org/10.1007/s11433-014-5466-5
16. Q. Y. Wang, M. Perc, Z. S. Duan, G. R. Chen, Delay-enhanced coherence of spiral waves in noisy Hodgkin-Huxley neuronal networks, *Phys. Lett. A*, **372** (2008), 5681–5687. https://doi.org/10.1016/j.physleta.2008.07.005
17. C. N. Takembo, A. Mvogo, H. P. E. Fouda, T. C. Kofane, Effect of electromagnetic radiation on the dynamics of spatiotemporal patterns in memristor-based neuronal network, *Nonlinear Dynam.*, **95** (2019), 1067–1078. https://doi.org/10.1007/s11071-018-4616-0
18. K. Rajagopal, A. Karthikeyan, S. Jafari, F. Parastesh, C. Volos, I. Hussain, Wave propagation and spiral wave formation in a Hindmarsh-Rose neuron model with fractional-order threshold memristor synaps, *Int. J. Mod. Phys. B*, **34** (2020), 2050157. https://doi.org/10.1142/S021797922050157X
19. H. Bao, B. C. Bao, Y. Lin, J. Wang, H. G. Wu, Hidden attractor and its dynamical characteristic in memristive self-oscillating system, *Acta Phys. Sin-Ch. Ed.*, **65** (2016), 180501. https://doi.org/10.7498/aps.65.180501

20. L. Chua, Resistance switching memories are memristors, *Appl. Phys. A-Mater.*, **102** (2011), 765–783. https://doi.org/10.1007/s00339-011-6264-9